Eur. Phys. J. D **8**, 211–222 (2000)

THE EUROPEAN PHYSICAL JOURNAL D

EDP Sciences

A theoretical spectroscopic study of single ammonia molecules adsorbed on the surface of fcc-type argon clusters. Surface effects on the ν_2 vibration-inversion mode

A. Lakhlifi[a]

Laboratoire d'Astrophysique de l'Observatoire de Besançon[b], 41 bis avenue de l'Observatoire, B.P. 1615, Université de Franche-Comté, 25010 Besançon Cedex, France

Received 6 April 1999 and Received in final form 19 July 1999

Abstract. Ammonia monomers have been adsorbed on argon clusters at low temperature $T \simeq 30$ K by Rohmund and Huisken [1] using the *pick-up* technique. They measured the spectrum of the NH_3 molecules in the region of the ν_2 umbrella mode. Two broad bands centered around 970 and 1000 cm^{-1} with finer details were observed. The authors attempted to interpret the obtained spectrum on the basis of the free rotation motions of the molecules. In this paper semi-empirical atom-atom potential energy calculations are performed for the ammonia monomer adsorbed on a rigid face-centered-cubic (*fcc*)-type surface of the argon cluster. In the equilibrium position of the rigid molecule on the cluster surface the orientational potential energy surface exhibits two quasi-equivalent minima separated by a potential barrier of about 100 cm^{-1}. The symmetry of the molecular vibration-inversion double-well potential is destroyed; the inversion motion is then forbidden in the ground state. On the basis of the two adsorption orientations, the vibrational frequency shifts are calculated and the obtained infrared bar-spectrum agrees with the experimental one.

PACS. 33.20.-t Molecular spectra – 33.20.Ea Infrared spectra – 33.20.Vq Vibration-rotation analysis

1 Introduction

Matrix isolation spectroscopy of chromophore atoms, molecules or radicals has been extensively developed, both experimentally and theoretically, to obtain information on the local structure of the trapping sites, the interaction potentials and their effects on the physical and chemical properties of the isolated species, in particular on their changes with respect to the gas phase state.

Rare gas (RG = Ar, Kr, Xe) solids, because of their chemically and spectroscopically inert character and their relatively weak and well studied van der Waals forces, have been widely used as matrices for isolating chromophores.

Since the eighties, increasing attention has been given to spectroscopic studies of chromophore molecules or small complexes embedded in, or adsorbed on, large RG host clusters which represent an intermediate state of the chromophores between the free gas phase and the trapped phase in the bulk matrix.

Two methods for producing the chromophore-cluster complex are used; the conventional *coexpansion* of a dilute mixture containing the chromophore molecules and the rare gas atoms, and the *pick-up* technique, invented in 1985 by Gough and co-workers [2], where one or several chromophore molecules are deposited on the surface of the previously formed RG clusters. These techniques permit the study at the microscopic level of both the dynamics and the chemical reactions of the adsorbed species.

Infrared (IR) spectroscopy experiments in the frequency range 900–1100 cm^{-1}, using the radiation of the line-tunable CO_2 lasers, have been carried out by Scoles and co-workers [2–8] for various molecules (SF_6, SiF_4, CH_3F, CF_3Cl, and CH_3CN) embedded in, or adsorbed on, solid argon Ar_n clusters ($n \leq 1000$). By comparing the spectra obtained with the pick-up and coexpansion techniques for different cluster sizes, the authors were able to characterize the location sites of the guest molecules *onto* or *inside* the clusters. Furthermore, the SF_6 molecule has been recently used as a microscopic probe to obtain information on the structural evolution of RG clusters as a function of their size [9]. Other experiments using the pick-up technique have been performed to study the spectroscopy of Ba atoms and their reaction with N_2O molecules, on the surface of large solid Ar_n clusters [10,11].

Theoretical calculations of the line shifts and structures of SF_6Ar_n and SiF_4Ar_n cluster systems as a function of n were carried out by Eichenauer and Le Roy [12] and Perera and Amar [13]. Perturbation theory was used to determine the frequency shifts for the ν_3 vibrational

[a] *Also at:* Institut Universitaire de Technologie of Belfort-Montbéliard. e-mail: azzedine.lakhlifi@obs-besancon.fr or iut-bm.univ-fcomte.fr

[b] UPRES A CNRS 6091

mode of SF_6 and SiF_4 chromophores. The authors concluded that the experimental results can be explained by assuming a dominant contribution from the instantaneous dipole-induced dipole interaction.

On the other hand, molecular dynamics simulations have been carried out by Gaigeot and co-workers [14] to study diffusion and clustering phenomena of N_2O molecules deposited by collision on Ar_{147} and Ar_{125} clusters. After each molecules-clusters collision, several quantities were calculated using simulation durations of ~ 40–120 ns. The results indicated a very high mobility and fast clustering of the molecules on the argon clusters.

Recently, Huisken *et al.* reported IR spectra of CH_3OH [15] and NH_3 [1] molecules (monomers and small polymers) adsorbed on medium-sized Ar_n clusters ($\langle n \rangle \sim 75$) at low temperatures ($T \simeq 30$ K). It was established that the molecules remain attached to the clusters for ~ 670 μs between the pick-up region and the spectroscopic detector.

Given the relative time scales involved in the above effects, we regard it as justified to treat the molecule as being in a state of thermal equilibrium.

Under the monomer conditions (see Tab. II in Ref. [1]), the measured spectrum for the NH_3 molecule concerns the ν_2 vibration-inversion mode in the frequency range 920–1060 cm^{-1}. It exhibits two broad bands with some finer details. These bands have maxima around 970 and 1000 cm^{-1}, and are separated by a minimum at 985 cm^{-1}. The authors of reference [1] tried to explain the two bands on the basis of the inversion motion and to assign the finer details to the free rotational transitions of the molecule, and they found a reduction of the inversion splitting from ~ 37 cm^{-1} in the gas phase to ~ 15 cm^{-1} for the adsorbed molecule.

During the eighties, many theoretical studies of the IR spectroscopy of ammonia molecules trapped in rare gas (Ar, Kr, Xe) and nitrogen matrices at low temperatures were carried out [16–21]. The question of the behaviour of the inversion splitting in different matrices was also investigated. In fact, owing to the symmetry of the trapping site, the double-well potential function associated with the vibration-inversion motion remains symmetric but its barrier height increases with respect to that for the gas phase.

Recently, we have studied the adsorption of ammonia molecules on a MgO dielectric substrate [22]. In this case the ν_2 mode is strongly perturbed and blueshifted by around 80 cm^{-1}. One of the two wells disappears and the inversion motion is then forbidden.

In this paper we present a theoretical study of the ammonia monomer adsorbed on a rigid *fcc-type* surface of an argon cluster. In the next section we describe the adsorbate-substrate system and the interaction potential model used in the calculations. In Section 3, the total Hamiltonian connected to the optical modes is treated, using a renormalization method to separate the different motions from each other. The frequency shifts of the ν_2 vibration mode and the orientational level scheme are then calculated and the surface effect on the NH_3 inversion motion is treated in detail. Finally, Sections 4 and 5 are devoted to the construction of the infrared bar-spectrum and to a discussion of the model, the effect of the cluster size on the results and the improvements which could be made to calculate the profile spectrum.

2 Structure and potential model

2.1 The ammonia molecule-argon cluster system

Experimental and theoretical investigations of the structures of pure Lennard-Jones (LJ) clusters have been reported frequently (see Ref. [23] for a bibliography). The number of atoms which constitute the cluster plays an important role in determining its equilibrium structure.

For argon, when $n \sim 75$ (which corresponds to the experimental ammonia-cluster size system in Ref. [1]), Farges *et al.* [24] and Northby [25] found a so called "twin" structure for $n \leq 70$ and a "regular" structure for $n \geq 82$. The two structures were found to be energetically equivalent for $70 \leq n \leq 82$.

However, more recently, Wales *et al.* have reported several calculations of Lennard-Jones and Morse clusters containing up to 110 atoms [26,27]. In particular, they calculated the lowest-energy minima for the range $n = 70-79$ and found that at $n = 70$, 75 and 79 the energies of the icosahedral, decahedral and *fcc* structures were virtually identical.

In the present work we elaborate our model by considering the adsorption of the ammonia monomer on a rigid *fcc-type* surface of the argon cluster, of the type designated $79E$ in Figure 15 in reference [26]. In Figure 1 we give the geometrical characteristics of the molecule-cluster system.

2.2 Interaction potential

The interaction potential energy V_{MC} between the oblate symmetric top molecule NH_3 and the argon cluster is taken as the sum of 12-6 Lennard-Jones (LJ) atom-atom potentials characterizing the repulsion-dispersion contributions plus an induction part due to the interaction between the permanent electric multipoles of the molecule and their images created at the positions of the Ar atoms. It can be written as

$$V_{\mathrm{MC}} = \sum_j \sum_{i=1}^{4} 4\epsilon_{ij} \left\{ \left(\frac{\sigma_{ij}}{r_{ij}} \right)^{12} - \left(\frac{\sigma_{ij}}{r_{ij}} \right)^{6} \right\} - \frac{1}{2} \sum_j \alpha_j E_{\mathrm{M}j}^2, \quad (1)$$

where i and j characterize the ith atom of the molecule and the jth argon atom of the cluster, respectively; ϵ_{ij} and σ_{ij} are the mixed LJ potential parameters obtained from the usual Lorentz-Berthelot combination rules $\epsilon_{ij} = \sqrt{\epsilon_{ii}\epsilon_{jj}}$ and $2\sigma_{ij} = \sigma_{ii} + \sigma_{jj}$, $\mathbf{E}_{\mathrm{M}j}$ is the field generated by the molecular permanent electric multipoles ($\boldsymbol{\mu}_{\mathrm{M}}$, $\boldsymbol{\Theta}_{\mathrm{M}}$, ...) on the jth argon atom with isotropic polarizability α_j,

Table 1. Pure Lennard-Jones potential parameters, isotropic polarizability of the argon atoms and their interdistance, in one hand, and internal characteristics of the rigid ammonia molecule, in the other hand.

Atoms	Ar	N	H	Internal charact.[a]	NH_3
ϵ^{a} (meV)	10.41	3.29	2.13	q_M^e (Å)	1.016
σ^{a} (Å)	3.44	3.38	2.53	β_M^e (deg.)	68.0
α^{b} (Å^3)	1.64	-	-	μ_M^e (D)	1.476
a^{b} (Å)	3.75	-	-	Θ_M^e (DÅ)	−2.930
a^{c} (Å)	3.87	-	-	B (cm^{-1})	9.941
				C (cm^{-1})	6.309

[a] From reference [29] and references therein.
[b] From reference [35].
[c] This value corresponds to the equilibrium distance between argon atoms obtained from the $2^{1/6}\sigma$ expression.

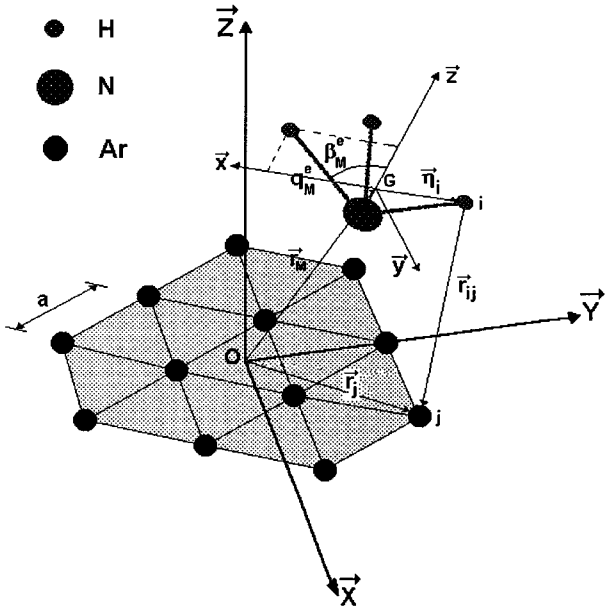

Fig. 1. Geometrical characteristics of the rigid NH_3 molecule absorbed on the *fcc*-type surface of the argon cluster. (**X, Y, Z**) and (**x, y, z**) are the surface absolute frame and the molecular frame, respectively. a is the distance between two nearest neighbor atoms in the argon cluster, q_M^e and β_M^e define the equilibrium N–H bond distance and H–N-**z** bond angle. Their values are given in Table 1.

and $\mathbf{r}_{ij}$ is the distance vector between the ith atom of the molecule and the jth Ar atom.

However, to establish the molecular orientational degrees of freedom $\boldsymbol{\Omega} = (\varphi, \theta, \chi)$ (precession, nutation, and proper rotation angles), the position vectors of the molecular centre of mass and the Ar atoms, we define an absolute frame (**X, Y, Z**) connected to the surface of the cluster, as described in Figure 1. The rotational matrix transformation from this absolute frame to the molecular frame (**x, y, z**) is given in Appendix A [28]. Note that the **z**-axis corresponds also to the C_3 symmetry axis of the symmetric top molecule. Thus the distance vector $\mathbf{r}_{ij}$ can be expressed in terms of the position vectors $\mathbf{r}_M = (X, Y, Z)$ and $\mathbf{r}_j$ of the molecular centre of mass and the jth argon atom, with respect to the absolute frame, and of the position vector $\boldsymbol{\eta}_i$ of the ith atom of the molecule with respect to its frame (**x, y, z**), as

$$\mathbf{r}_{ij} = \mathbf{r}_j - \mathbf{r}_M - \boldsymbol{\eta}_i. \tag{2}$$

In Table 1 we give the internal characteristics of the rigid NH_3 molecule in the gas phase state, the isotropic polarizability α, the equilibrium distance a between two nearest neighbor atoms in our rigid argon cluster, and the pure atom-atom $\{\epsilon, \sigma\}$ LJ potential parameters. The values of these parameters have been considerably refined in our previous spectroscopic studies of the ammonia molecules trapped in rare gas matrices [16–19,29].

In order to study the influence of the surroundings on the molecular internal motions, the position vectors $\boldsymbol{\eta}_i$ of the atoms in the molecule and the molecular dipole vector $\boldsymbol{\mu}_M$ and quadrupole tensor $\boldsymbol{\Theta}_M$ moments, can be expressed, with respect to the molecular frame, in terms of the vibrational normal coordinates Q as

$$\begin{aligned} \boldsymbol{\eta}_i &= \boldsymbol{\eta}_i^e + \sum_\lambda \mathbf{a}_i^\lambda Q_\lambda, \\ \boldsymbol{\mu}_M &= \boldsymbol{\mu}_M^e + \sum_\lambda \mathbf{b}_M^\lambda Q_\lambda, \\ \boldsymbol{\Theta}_M &= \boldsymbol{\Theta}_M^e + \sum_\lambda \mathbf{c}_M^\lambda Q_\lambda. \end{aligned} \tag{3}$$

In these expressions the superscript e characterizes the internal equilibrium configuration of the molecule, Q_λ is the normal coordinate connected to the λth vibrational mode with frequency ω_λ, and $\mathbf{a}_i^\lambda$, $\mathbf{b}_M^\lambda$, and $\mathbf{c}_M^\lambda$ are the first derivatives, with respect to Q_λ, of $\boldsymbol{\eta}_i$, $\boldsymbol{\mu}_M$, and $\boldsymbol{\Theta}_M$, respectively. Their components in the molecular frame are given elsewhere [30].

2.3 Separation of V_{MC}

As already mentioned, we are interested in calculating the frequency shifts and IR bar-spectrum, in the ν_2 mode region, of NH_3 monomers adsorbed on the surface of argon clusters. The broadening mechanisms and energy transfers

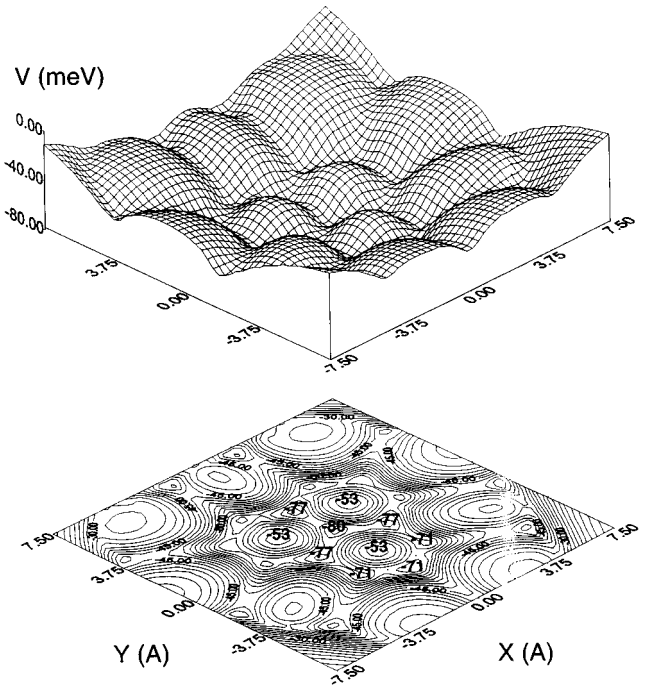

Fig. 2. Minimum potential energy surface $V_{\rm M}$ *versus* the (X, Y) laterally position of the centre of mass of the NH_3 molecule above the surface of argon cluster. Lower surface labels the isoenergetic curves.

are then ignored, assuming that the dynamical coupling between the degrees of freedom is negligible. Therefore one can consider the cluster as being rigid and use the adiabatic approximation to separate the high frequency vibrational modes of the molecule from its low frequency external modes. The interaction potential energy $V_{\rm MC}$ can be written as

$$V_{\rm MC} = V_{\rm M}(\mathbf{r}_{\rm M}, \boldsymbol{\Omega}) + W_{\rm M}(\{Q\}), \tag{4}$$

where $V_{\rm M}(\mathbf{r}_{\rm M}, \boldsymbol{\Omega})$ represents the external motion dependent part of the potential for the rigid molecule and $W_{\rm M}(\{Q\})$ characterizes the vibrational dependent part for the molecule at its equilibrium position and orientation.

In Figure 2 we present the potential energy surface $V_{\rm M}(X, Y)$ experienced by the rigid ammonia molecule as it moves laterally above the surface of the argon cluster. For each (X, Y) molecular position, $V_{\rm M}$ is minimized with respect to the perpendicular distance Z and the angular coordinates (φ, θ, χ). The surface of the cluster appears moderately corrugated around the central regular triangle. The more favourable adsorption site ($V_{\rm M}^{\rm e} = -80$ meV) is located at $X^{\rm e} = Y^{\rm e} = 0$ for a perpendicular distance $Z^{\rm e} = 3$ Å and an orientation position $\varphi^{\rm e} = 0, \theta^{\rm e} = \pi, \chi^{\rm e} = \pi/2$, in which the H atoms are close to the surface and point perpendicularly each one to one side of the central triangle. The adsorption energy for the molecule above the three argon atoms of this triangle is -53 meV obtained for the same orientation and the distance $Z = 3.5$ Å.

On the isoenergetic curves (lower surface) of Figure 2, we give also the minimum values of $V_{\rm M}(X, Y)$ obtained for the more favourable sites of the three neighbor triangles ($V_{\rm M} = -77$ meV) and the next most favourable ones ($V_{\rm M} = -71$ meV). Note, however, that the energy barriers for the NH_3 diffusion valleys between two adjacent favourable sites are equal to 7.5 meV, and the diffusion constant has been estimated as $\sim 2 \times 10^{-5}$ cm^{2}s^{-1}. Moreover, as the molecule approaches the surface edges, it experiences a retarding force with an associated energy value of about -40 meV. Such edge sites do not correspond to probable adsorption sites and the molecule does not desorb from the surface of the cluster. This phenomenon is so-called *Schwoebel's effect*.

Finally, to study the optically active modes (vibration and orientation modes) of the ammonia molecule, we will assume it to be adsorbed at its laterally equilibrium position $X^{\rm e} = Y^{\rm e} = 0$ and will replace $V_{\rm M}(\mathbf{r}_{\rm M}, \boldsymbol{\Omega})$ in the next section by $V_{\rm M}(\boldsymbol{\Omega})$ minimized, for each set of $\boldsymbol{\Omega} = (\varphi, \theta, \chi)$ values, with respect to the perpendicular distance Z.

3 Quantum mechanical model

3.1 Renormalized total Hamiltonian

Under the conditions considered before, the optical system is defined to involve the molecular vibrations and the orientation motions only. The associated Hamiltonian can then be written

$$H_{\rm M} = T_{\rm rot} + H_{\rm vib} + V_{\rm M}(\boldsymbol{\Omega}) + W_{\rm M}(\{Q\}), \tag{5}$$

where $T_{\rm rot}$ is the rotational kinetic Hamiltonian for the free symmetric top molecule expressed in terms of the orientational degrees of freedom (φ, θ, χ) with respect to the absolute frame [31]

$$T_{\rm rot} = -B \left\{ \frac{\partial^2}{\partial\theta^2} + \cot\theta \frac{\partial}{\partial\theta} + \frac{1}{\sin^2\theta} \frac{\partial^2}{\partial\varphi^2} + \left(\cot^2\theta + \frac{C}{B} \right) \frac{\partial^2}{\partial\chi^2} - 2\frac{\cot\theta}{\sin\theta} \frac{\partial^2}{\partial\varphi\partial\chi} \right\}. \tag{6}$$

B and C are the rotational constants for the motion of the molecular C_3 symmetry axis and the motion around this axis, respectively. Their values for the rigid NH_3 are given in Table 1.

In equation (5), $H_{\rm vib}$ is the internal vibrational Hamiltonian of the NH_3 gas phase state. Its expression is

$$H_{\rm vib} = \sum_{\lambda} \frac{P_\lambda^2}{2\mu_\lambda} + V_{\rm vib}(\{Q\}), \tag{7}$$

where μ_λ and $\mathbf{P}_\lambda$ are the reduced mass and the conjugate momentum operator, connected to the λth vibrational mode with normal coordinate Q_λ and frequency ω_λ. The normal coordinates are assumed to be small displacements with respect to the internal equilibrium configuration of the molecule. The second term $V_{\rm vib}(\{Q\})$ represents the internal potential energy surface that is generally given as a Taylor series expansion with respect to the Q normal

$$\sum_{JMK} \Lambda^{jmk}_{JMK} \sum_{J'M'K'} \left\{ \begin{array}{c} (E_{J'M'K'} - E_{j'm'k'})\,\delta_{J,J'}\delta_{M,M'}\delta_{K,K'} \\ + \left(\frac{2J+1}{2J'+1}\right)^{\frac{1}{2}} \sum_{lpq} A^{l}_{p,q} C(JlJ';MpM') C(JlJ';KqK') \end{array} \right\} \Lambda^{j'm'k'}_{J'M'K'} = 0, \quad (13)$$

coordinates. It can be separated into harmonic (up to second order) part, with force constant K_λ, and anharmonic (higher orders) one

$$V_{\rm vib}(\{Q\}) = \sum_{\lambda} \frac{1}{2} K_\lambda Q^2_\lambda + \Delta V^{\rm anh}_{\rm vib}(\{Q\}). \quad (8)$$

For the calculation of the vibrational frequency shifts of the adsorbed molecule, the eigenelements of the vibrational Hamiltonian $H_{\rm vib}$ are needed. By assuming the anharmonic part as small perturbation, the eigenvectors can be written, on the basis of the harmonic eigenvectors $|v_\lambda\rangle$, as [30]

$$|v_1 v_2 v_{3a} v_{3b} v_{4a} v_{4b}\rangle = \sum_{v'_1,\ldots,v'_{4b}} \Gamma^{v'}_{v} |v'_1\rangle \ldots |v'_{4b}\rangle, \quad (9)$$

where v and v' are the vibrational quantum numbers and Γ the resulting coefficients from the first order perturbation treatment. Note that the vibrational potential energy surface, used in our calculations for the gas phase NH_3, is obtained from *ab initio* calculations of Martin *et al.* [32].

Finally the orientational and vibrational parts of the interaction potential, given in equation (5), will be introduced below to renormalize the rotational and vibrational Hamiltonians of the gas phase molecule, respectively.

3.2 Angular motions

The orientational potential energy surface $V_{\rm M}(\varphi,\theta,\chi)$, experienced by the non vibrating NH_3 molecule at its adsorption site, has been numerically calculated. It exhibits not the free rotation behaviour but moderately hindered angular motions. Two minima were obtained for $\theta = 0$ and $\theta = \pi$ ($\varphi = 0, \chi = \pi/2$) orientation positions with energies $V_{\rm M} = -75.9$ and -80 meV, respectively. The energy barrier for the minimum valley between these two orientations is equal to 14 meV, the φ, θ, and χ angular motions being relatively strongly coupled. Note however that the energy difference between the potential surface maxima and minima can reach 23 meV, and the Z distance values which minimize this $V_{\rm M}(\varphi,\theta,\chi)$ surface are found to be between 2.9 and 3.2 Å.

Thus the Schrödinger equation associated with the orientational Hamiltonian for the adsorbed ammonia,

$$\begin{aligned} &H_{\rm orient}|jmk\rangle = E_{jmk}|jmk\rangle, \\ &H_{\rm orient} = T_{\rm rot} + V_M(\varphi,\theta,\chi), \end{aligned} \quad (10)$$

can be solved on the basis of the eigenelements connected to the free rotation of the oblate symmetric top molecule. Let E_{JMK} and $|JMK\rangle$ be these eigenelements in which J, M, and K are the usual rotational quantum numbers [31]. The eigenkets $|jmk\rangle$ connected to $H_{\rm orient}$ can be expanded as linear combinations

$$|jmk\rangle = \sum_{JMK} \Lambda^{jmk}_{JMK} |JMK\rangle, \quad (11)$$

where Λ will be the resulting coefficients which are complex numbers obtained by solving the system of secular equations given below. To establish these equations, $V_{\rm M}(\varphi,\theta,\chi)$ has been fitted on the basis of the $D(\varphi,\theta,\chi)$ Wigner rotation elements [28] as

$$V_{\rm M}(\varphi,\theta,\chi) = \sum_{lpq} A^{l}_{p,q} D^{l}_{p,q}(\varphi,\theta,\chi). \quad (12)$$

In this expression $l = 0, 1, \ldots$ is an integer number connected to the θ angle, while p and q are connected to the φ and χ angles, respectively, and can take the values $0, \pm 1, \ldots, \pm l$. Note however that, because of the C_{3v} symmetry of the molecule, the q number can only take values which are multiples of 3, including zero. In equation (12) the $A^l_{p,q}$ fitting coefficients are complex numbers which have been calculated up to $l = 8$. The higher expansion terms were negligibly small.

Finally, the system of secular equations to be solved is

see equation (13) above

where δ and C are the Kronecker symbols and the Clebsch-Gordan coefficients which appear after applying the addition theorem of the $D(\varphi,\theta,\chi)$ elements [28]. Equation (13) are then solved by diagonalizing a sparse characteristic matrix of 1771×1771 minimum dimension that allows terms in equation (12) up to $l = 8$ to perturb levels up to $j = 0, 1, 2$. Higher jmk levels are negligibly populated at temperature $T \simeq 30$ K and large precision in their calculation is not required.

In Figure 3 we give the calculated orientational level scheme up to $j = 2$; and for comparison, in the lower part, the corresponding free rotational levels (dashed levels). It can be seen that the orientational levels exhibit splittings due to the lifting of the degeneracy of the magnetic m and spinning k quantum numbers. Moreover the obtained Λ coefficients indicate that the eigenvectors $|jmk\rangle$ (see Eq. (11)) result from a strong perturbation of the free $|JMK\rangle$ rotation states due to the orientational potential energy surface. They will be used to calculate the orientational transition elements for the infrared spectrum.

3.3 Vibrational level energy shifts

The vibrational dependent part $W_{\rm M}(\{Q\})$, of equation (5), is generally a small perturbation which can

Table 2. Linear combination coefficients of the $|v_2^{(\alpha)}\rangle$ vibration-inversion wavefunctions in terms of the $|v_2^{(\mathrm{L})}\rangle$ and $|v_2^{(\mathrm{R})}\rangle$ ones connected to the left and right wells, respectively.

	Gas NH_3		Adsorbed NH_3	
$\|v_2^{(\alpha)}\rangle$	$\|v_2^{(\mathrm{L})}\rangle$	$\|v_2^{(\mathrm{R})}\rangle$	$\|v_2^{(\mathrm{L})}\rangle$	$\|v_2^{(\mathrm{R})}\rangle$
$\|0^{(+)}\rangle$	$+1/\sqrt{2}$	$+1/\sqrt{2}$	$+0.010$	~ 1
$\|0^{(-)}\rangle$	$+1/\sqrt{2}$	$-1/\sqrt{2}$	~ 1	-0.010
$\|1^{(+)}\rangle$	$+1/\sqrt{2}$	$+1/\sqrt{2}$	$+0.579$	$+0.816$
$\|1^{(-)}\rangle$	$+1/\sqrt{2}$	$-1/\sqrt{2}$	$+0.795$	-0.606

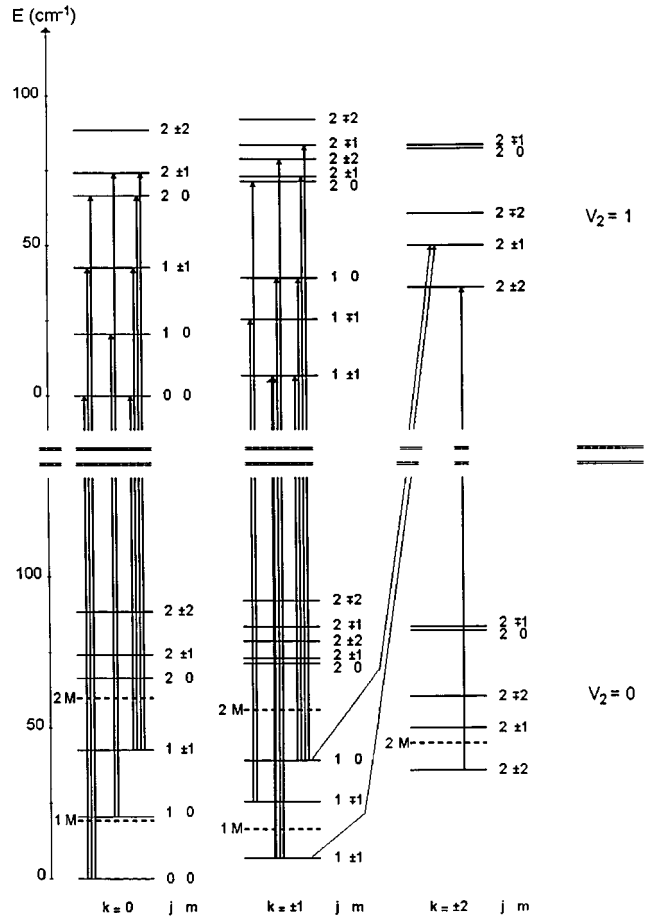

Fig. 3. Orientation level scheme of the rigid ammonia molecule adsorbed, at its laterally equilibrium position, on the surface of argon cluster (solid levels). For comparison the free rotation level scheme is also given (dashed levels). The arrows label the non negligible transitions used in the bar-spectrum calculations.

involve level shifts and/or splittings, only. It can be developed as a Taylor expansion up to second order with respect to the vibrational normal coordinates Q. One can write

$$W_{\mathrm{M}}(\{Q\}) = \sum_{\lambda} \left(\frac{\partial V_{\mathrm{MC}}}{\partial Q_\lambda}\right)^{\mathrm{e}} Q_\lambda + \sum_{\lambda \le \lambda'} \left(\frac{\partial^2 V_{\mathrm{MC}}}{\partial Q_\lambda \partial Q_{\lambda'}}\right)^{\mathrm{e}} Q_\lambda Q_{\lambda'} \qquad (14)$$

where the e-superscripted terms represent the first and second derivatives of the interaction potential energy with respect to the vibrational coordinates and are calculated for the equilibrium geometry of the molecule on the clusters surface.

Let E_{v_λ} and $|...v_\lambda...\rangle$ be the anharmonic eigen-energy and vector of the vth level connected to the λth vibrational mode and obtained previously. Using a first order perturbation treatment, the energy level shift ΔE_{v_λ} for the adsorbed molecule can be calculated from

$$\Delta E_{v_\lambda} = \langle ...v_\lambda...|W_M|...v_\lambda...\rangle, \qquad (15)$$

in which all other modes remain in their fundamental states. Note that to this order of the perturbation treatment, the eigenvectors do not change.

3.4 Ammonia ν_2 mode

3.4.1 Free NH_3

In the ν_2 vibration-inversion mode of the free NH_3, the hydrogen atoms can pass from one side of the nitrogen atom to the other. This is generally described, to a good approximation, as one-dimension tunnelling motion of one particle in a symmetrical double-well potential function (left (L) and right (R) wells) with a high, but finite, hindering barrier [33]. The solution of such problem leads to vibrational energy levels split into doublets, (+) and (−), due to inversion. The vibration-inversion wavefunctions are then described by $|v_2^{(\alpha)}\rangle$ ($\alpha = +, -$), instead of $|v_2\rangle$, and can be expressed as linear combinations (symmetric and antisymmetric) of the vibrational wavefunctions $|v_2^{(\mathrm{L})}\rangle$ and $|v_2^{(\mathrm{R})}\rangle$ associated with the left and right wells. Table 2 gives the combination coefficients for the fundamental and first excited states. Moreover, the values of the $\left|\langle v_2^{(\alpha)}|Q_2|v_2^{\prime(\alpha')}\rangle\right|$ elements indicate that only transitions with inversion motion can take place as given in Table 3.

3.4.2 Adsorbed NH_3

When the NH_3 molecule is adsorbed on the argon cluster, the two equilibrium positions of the hydrogen atoms with respect to the nitrogen atom correspond to the $\theta = 0$ and $\theta = \pi$ angular positions, with the energies -75.9

Table 3. Elements (Å) of the vibration-inversion normal coordinate Q_2 for ammonia molecule in the gas phase and adsorbed on the surface of argon cluster.

		Gas NH_3	Adsorbed NH_3
$\|v_2^{(\alpha)}\rangle$	$\|v_2'^{(\alpha')}\rangle$	$\|\langle v_2^{(\alpha)}\|Q_2\|v_2'^{(\alpha')}\rangle\|$	$\|\langle v_2^{(\alpha)}\|Q_2\|v_2'^{(\alpha')}\rangle\|$[a]
$\|0^{(+)}\rangle$	$\|0^{(+)}\rangle$	~ 0	0.374
	$\|0^{(-)}\rangle$	0.372	~ 0
	$\|1^{(+)}\rangle$	~ 0	0.066
	$\|1^{(-)}\rangle$	0.081	0.048
$\|0^{(-)}\rangle$	$\|0^{(-)}\rangle$	~ 0	0.373
	$\|1^{(+)}\rangle$	0.083	0.049
	$\|1^{(-)}\rangle$	~ 0	0.066
$\|1^{(+)}\rangle$	$\|1^{(+)}\rangle$	~ 0	0.220
	$\|1^{(-)}\rangle$	0.323	0.238
$\|1^{(-)}\rangle$	$\|1^{(-)}\rangle$	~ 0	0.218

[a] In the following, these elements will be replaced by $|\langle v_2^{(\Theta)}|Q_2|v_2'^{(\Theta')}\rangle|$ where Θ and Θ' define the left L or/and right R wells.

and −80 meV, respectively. Because of the non-free rotation the vibration-inversion double-well potential function acquires an asymmetry with energy difference $\Delta =$ 4.1 meV. This potential function is shown in Figure 4 *versus* the angle between the N–H bond and the plane of the H atoms.

The corresponding Schrödinger equation was solved numerically using a discrete variable representation method [34]. The first four energy levels and their wavefunctions are also drawn in Figure 4, and the resulting combination coefficients are then given in Table 2. They indicate that the wavefunctions $|0^{(+)}\rangle$ and $|0^{(-)}\rangle$ simply become $|0^{(\mathrm{R})}\rangle$ and $|0^{(\mathrm{L})}\rangle$, respectively.

At this stage, some important remarks could be made:

(i) the ammonia molecule can adsorb on the site surface about the $\theta = 0$ or $\theta = \pi$ orientation position, which amounts to finding it in the left (L) or right (R) well of Figure 4;

(ii) in the fundamental vibrational state there is no inversion motion since the transition element between the $|0^{(\mathrm{R})}\rangle$ and $|0^{(\mathrm{L})}\rangle$ states is negligibly small as given in Table 3. Note however, that the molecule can leak between the first excited states because of their energy levels positions with respect to the top of the barrier;

(iii) when the molecule undergoes near infrared excitation $v_2 = 0 \rightarrow v_2 = 1$, the transition can take place with or without inversion motion. In effect, the two corresponding transition elements are not zero (see Tab. 3);

(iv) finally the vibrational dependent part $W_{\mathrm{M}}(\{Q\})$ (Eq. (14)) due to the surroundings will be quite different if the molecule is in the left well or in the right one (*i.e.* at $\theta = 0$ or $\theta = \pi$). Then, $W_{\mathrm{M}}(\{Q\})$ will be replaced in equation (15) by the parametrically dependent $W_{\mathrm{M}}^{(\Theta)}(\{Q\})$ in which Θ means the left L or right R well.

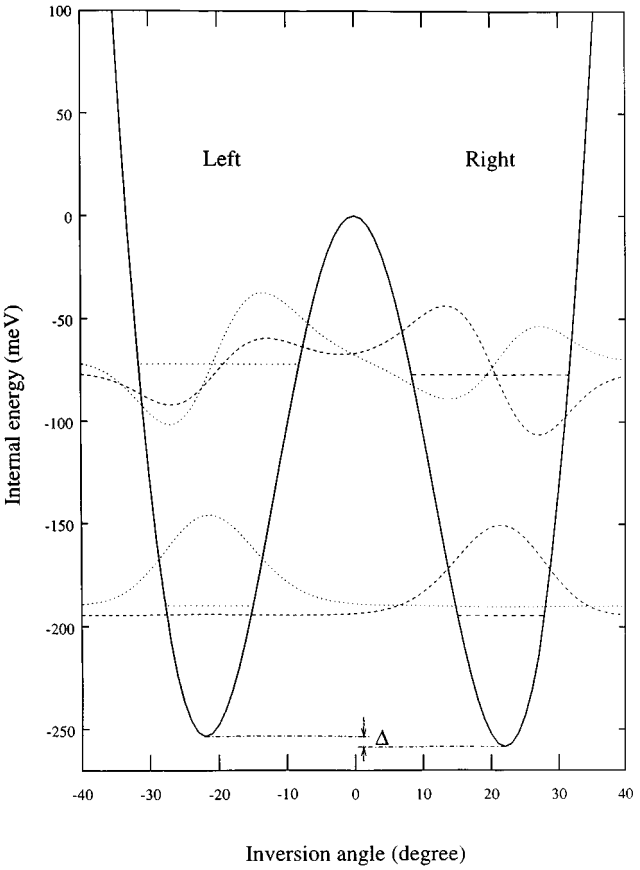

Fig. 4. Asymmetric vibration-inversion double-well potential, of NH_3 adsorbed on the surface of argon cluster, *versus* the angle between the N–H bond and the plane of the H atoms. $\Delta = 4.1$ meV characterizes the energy difference between the two wells. The obtained eigenenergy levels and their associated wavefunctions are also drawn.

4 Infrared spectrum

4.1 Absorption coefficient

The infrared absorption coefficient for a number $\mathcal{N}$ of active molecules is defined by

$$I(\omega) = \frac{4\pi\omega\mathcal{N}}{3hc}\mathrm{Re}\int_0^\infty \mathrm{d}t\mathrm{e}^{-\mathrm{i}\omega t}\mathrm{Tr}\left[\boldsymbol{\mu}_\mathrm{A}(0)\boldsymbol{\mu}_\mathrm{A}(t)\rho(0)\right], \quad (16)$$

where ω is a running frequency and c the light velocity in the vacuum, $\rho(0)$ characterizes the initial canonical density matrix associated with the total system, and $\boldsymbol{\mu}_\mathrm{A}$ is the molecular dipole moment expressed in the surface absolute frame (see Appendix A). The symbol Re defines the real part of the Fourier transform of the molecular dipole time correlation and the trace (Tr) operation means an average over the time evolution of the system.

As mentioned above, this work is devoted to constructing the infrared bar-spectrum of ammonia monomers adsorbed on the surface of argon clusters. The calculations are performed within the following assumptions and approximations:

(i) the ammonia-cluster systems are assumed to be isolated from each other *i.e.* the possible interaction between ammonia molecules is ignored. Therefore, no inhomogeneous broadenings of the infrared spectrum lines may exist;
(ii) the initial chaos hypothesis for the density matrix is assumed to be valid. This allows the optical states $|...v_\lambda...jmk\rangle$ to be written as the products of the renormalized vibrational and orientational states $|...v_\lambda...\rangle \times |jmk\rangle$;
(iii) and, as we have seen above, two adsorption orientation positions are possible. This allows the number $\mathcal{N}$ of active molecules defined in equation (16) to be written as the sum $\mathcal{N}^{(\mathrm{L})} + \mathcal{N}^{(\mathrm{R})}$ of the numbers of adsorbed molecules at $\theta = 0$ (left well) and $\theta = \pi$ (right well) orientations, respectively.

Within these approximations, the integrated absorption coefficient connected to the λth vibrational fundamental transition $|0_\lambda^{(\Theta)}\rangle \rightarrow |1_\lambda^{(\Theta')}\rangle$ (all other modes are in their fundamental states) with frequency $\omega_\lambda = \hbar^{-1}\left(E_{1_\lambda} - E_{0_\lambda}\right)$ and frequency shift $\Delta\omega_\lambda^{(\Theta\rightarrow\Theta')} = \hbar^{-1}\left(\Delta E_{1_\lambda}^{(\Theta')} - \Delta E_{0_\lambda}^{(\Theta)}\right)$ is written as

$$I_\lambda(\omega) = \frac{8\pi^2}{3hc}\omega \sum_{\Theta=\mathrm{L,R}}\sum_{\Theta'=\mathrm{L,R}} \mathcal{N}^{(\Theta)}\left|\left\langle 0_\lambda^{(\Theta)}\left|Q_\lambda\right|1_\lambda^{(\Theta')}\right\rangle\right|^2 \times \sum_{\substack{jmk\\ j'm'k'}} \frac{\mathrm{e}^{-\beta E_{jmk}}}{Z^{(\Theta)}}\left|\left\langle jmk\left|\frac{\partial\boldsymbol{\mu}_\mathrm{A}}{\partial Q_\lambda}\right|j'm'k'\right\rangle\right|^2 \times \delta\left(\omega - \omega_\lambda - \Delta\omega_\lambda^{(\Theta\rightarrow\Theta')} - \hbar^{-1}\left(E_{j'm'k'} - E_{jmk}\right)\right). \quad (17)$$

In this equation the $\langle ...\rangle$ brackets represent the transition elements of the normal coordinate Q_λ, on the one hand, and of the first derivative of the molecular dipole moment with respect to this coordinate, expressed in the absolute frame (see Appendix A), on the other hand. E_{jmk} and $E_{j'm'k'}$ are the eigenenergies, obtained by solving equation (13), of the initial and final orientational states, $Z^{(\Theta)}$ defines the orientation canonical partition function connected to the fundamental vibrational levels at temperature T, $\beta = (k_\mathrm{B}T)^{-1}$, and δ is the Dirac function. In equation (17) the sums over Θ and Θ' exist for the ν_2 vibration-inversion mode, only. For the other vibrational modes the sum over Θ' must be ignored.

4.2 ν_2 infrared bar-spectrum

To calculate the integrated absorption coefficient, let $\mathcal{N}^{(\mathrm{R})} = \mathcal{N}^{(\mathrm{L})} = 50\mathcal{N}\%$ be the distribution of the optically active ammonia molecules in the $\theta = \pi$ and $\theta = 0$ adsorption orientations, respectively. This means that the molecules have the same probability to be adsorbed on the (R) site as on the (L) one.

On the one hand, the expressions of the vibrational dependent parts $W_\mathrm{M}^{(\mathrm{R})}(\{Q\})$ and $W_\mathrm{M}^{(\mathrm{L})}(\{Q\})$ for the adsorbed molecules, have been determined and, using equation (15), the energy level shifts calculated for the vibrational ground and first excited states $v_2 = 0$ and $v_2 = 1$. The obtained values, 6.2 and 24.9 cm^{-1} for $0^{(\mathrm{R})}$ and $1^{(\mathrm{R})}$ levels, and 2.6 and 2.7 cm^{-1} for $0^{(\mathrm{L})}$ and $1^{(\mathrm{L})}$ ones, indicate that ν_2 mode is quite strongly perturbed when the H atoms of the molecule are close to the surface and less so when they are further away from it. This means that the interaction between the H atoms and the surface is more repulsive for the $\theta = \pi$ orientation than for $\theta = 0$ one. In Table 4 we give the frequencies ω_2 (see also Fig. 4), the frequency shifts $\Delta\omega_2$ and the square elements of the normal coordinate Q_2, connected to the four possible vibrational transitions between the ground and first excited states. These results will be used in equation (17) for calculating the bar-spectrum.

On the other hand, the squared orientational transition elements connected to the first derivative, with respect to Q_2, of the molecular dipole moment (Appendix A), were calculated using the eigenvectors obtained by solving equation (13). Table 5 gives the orientational eigenenergies of the non negligibly populated initial states $|jmk\rangle$, at temperature $T \simeq 30$ K, and the final ones $|j'm'k'\rangle$ and their associated main squared transition elements. Nevertheless, it can be noted that no selection rules could be predicted for the orientation transitions as in the free rotation case.

By introducing the results of Tables 4 and 5 in equation (17), the integrated absorption coefficient has been calculated in the frequency range 920–1080 cm^{-1}. The arrows in Figure 3 represent the main vibration-orientation transitions for one of the four possible vibration transitions. Finally the obtained bar-spectrum is shown in Figure 5 and, for comparison, the experimental spectrum

Table 4. Vibration-inversion frequencies (cm^{-1}), frequency shifts (cm^{-1}) and squared transition elements ($Å^2$) of the normal coordinate Q_2 for ammonia adsorbed on the surface of argon cluster.

$\|0^{(\Theta)}\rangle$	→	$\|1^{(\Theta')}\rangle$	ω_2	$\Delta\omega_2$	$\left\|\langle 0^{(\Theta)}\|Q_2\|1^{(\Theta')}\rangle\right\|^2$
$\|0^{(R)}\rangle$	→	$\|1^{(R)}\rangle$	952.3	+18.7	4.36×10^{-3}
	→	$\|1^{(L)}\rangle$	999.7	−3.5	2.30×10^{-3}
$\|0^{(L)}\rangle$	→	$\|1^{(R)}\rangle$	913.1	+22.3	2.40×10^{-3}
	→	$\|1^{(L)}\rangle$	960.5	+0.1	4.36×10^{-3}

Table 5. Orientational energy levels (cm^{-1}) and squared transition elements ($D^2Å^{-2}$) of the first derivative of the molecular dipole moment of ammonia adsorbed on argon cluster. The levels jmk are the lower levels non negligibly populated at $T \simeq 30$ K.

jmk	E_{jmk}	→	$j'm'k'$	$E_{j'm'k'}$	$\left\|\left\langle jmk \left\| \frac{\partial \boldsymbol{\mu}_A}{\partial Q_2} \right\| j'm'k' \right\rangle\right\|^2$
000	0	→	000	0	11.36
		→	1±10	42.5	3.03
		→	200	66.6	2.13
1±1±1	6.2	→	1±1±1	6.2	12.04
		→	10±1	38.9	1.32
		→	2±1±2	49.8	1.61
		→	2±2±1	78.7	1.17
100	20.6	→	100	20.6	11.49
		→	2±10	74.0	2.43
1±1∓1	25.4	→	1±1∓1	25.4	12.67
		→	20∓1	70.9	1.82
2±2±2	35.7	→	2±2±2	35.7	13.10
10±1	38.9	→	1±1±1	6.2	1.25
		→	10±1	38.9	2.92
		→	2±1±2	49.8	0.98
		→	2±1±1	72.4	1.37
		→	2±1∓1	83.2	0.88
1±10	42.5	→	000	0	3.03
		→	1±10	42.5	3.42
		→	200	66.6	2.59
		→	2±10	74.0	3.03

of Huisken and Rohmund [1], for ammonia monomers adsorbed on argon clusters, is also drawn. In Figure 5 intensities are given in arbitrary units as percentages with respect to the more intense line.

In the bar-spectrum the four strongest bands at the frequency positions 935.4, 960.6, 971, and 996.2 cm^{-1} characterize pure vibration transitions $|0^{(\Theta)}\rangle \times |jmk\rangle \rightarrow |1^{(\Theta')}\rangle \times |jmk\rangle$ where $\Theta \rightarrow \Theta' \equiv$ L → R, L → L, R → R and R → L, respectively. These bands are themselves constituted of several lines which are due to the number of populated initial orientational states at the temperature we consider.

The other lines are connected to vibration-orientation transitions $|0^{(\Theta)}\rangle \times |jmk\rangle \rightarrow |1^{(\Theta')}\rangle \times |j'm'k'\rangle$ ($\Theta \rightarrow \Theta'$ are the same as above). Their intensity values are found to be between 2% and 35% the more intense line. They are essentially distributed in groups around 968, 980, 993, 1004 and 1014 cm^{-1}, and in the frequency range 1023–1043 cm^{-1}.

We note that transitions without inversion motion L → L and R → R are ∼2 times stronger than transitions with inversion motion L → R and R → L, due to the squared transition elements of the normal coordinate Q_2 as given in Table 4.

Finally the calculated bar-spectrum seems qualitatively in satisfactory good agreement with the experimental spectrum and interprets the experimentally observed trends in a quite different fashion from that in the matrix isolated or free NH_3 cases, with the removed symmetry of the surroundings around the molecule on its adsorption site playing the key role.

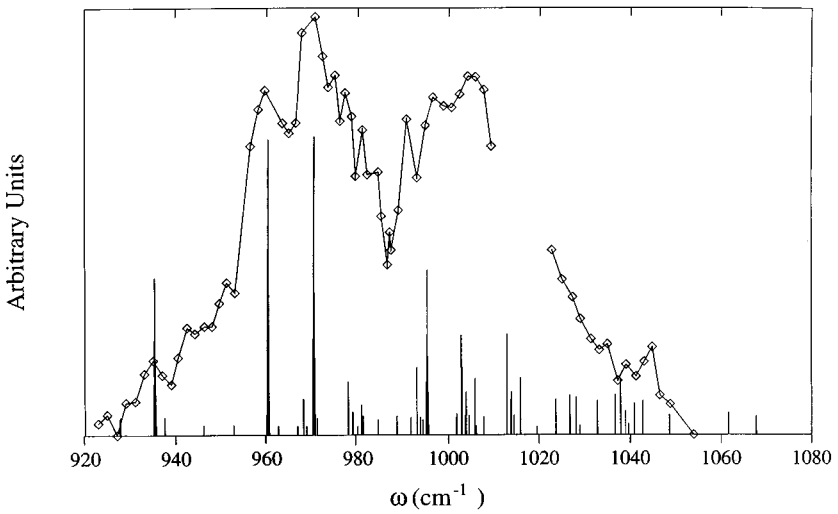

Fig. 5. Infrared spectra of ammonia monomers adsorbed on the surface of argon clusters, at $T \simeq 30$ K, in the vibration-inversion ν_2 region. Peaks characterize the bar-spectrum calculated in this work, for $\mathcal{N}^{(\mathrm{R})} = \mathcal{N}^{(\mathrm{L})}$ condition (see the text), and solid curve represents the experimental spectrum obtained by Rohmund and Huisken [1].

5 Discussion

The present calculations have used a particular model to study the adsorption processes of the ammonia monomer on the surface of an argon cluster. The interpretation of the available experimental spectrum of the chromophore in the ν_2 vibrational frequency region was made using some assumptions and approximations, the influence of which is discussed in this section.

To describe the interaction between the molecule and the cluster a semi-empirical atom-atom potential energy surface is used. The argon cluster is assumed to have a solid face-centered-cubic structure with a distance a between nearest neighbor atoms equal to the crystal phase one (see Tab. 1).

In order to evaluate approximately the influence of both the structure and size of the argon cluster on the potential energy surface V_{M} of the adsorbed molecule, we performed two calculations:

(i) on one hand, a distance $a = 3.870$ Å, corresponding to the equilibrium distance between two free interacting argon atoms, was introduced to take into account the non-crystalline structure of the cluster. The whole potential energy surface undergoes an absolute change of $\sim +2.5$ meV. The orientational energy barrier and the energy difference Δ connected to the asymmetry of the molecular vibration-inversion double-well potential (see Fig. 4), decrease by about 0.5 meV and 0.3 meV, respectively;

(ii) on the other hand, we used several increasing cluster sizes up to the semi-infinite substrate limit, for the adsorption of the molecule. In this last case the absolute change reaches -5 meV for the whole potential energy surface, and the orientational energy barrier and the energy difference Δ increase by about 0.5 meV and 0.2 meV, respectively.

These changes are very small compared to the orientational energy barrier of 14 meV and to the energy difference $\Delta = 4.1$ meV, obtained in the previous sections. One concludes that, in the rigid approximation, the changes of the structure and size of the cluster bring an extra modification of the molecular motions that is not significant.

Although we studied the $79E$ type structure given in reference [26], we note that the very small threshold value of Δ required to block the inversion motion in the ground vibrational state indicates that this blocking effect will be dominant even for other site symmetries for which slightly different parameter values are appropriate.

In Figure 5, the agreement between the calculated bar-spectrum and the experimental spectrum clearly shows the pertinence of the renormalization procedure developed in this theoretical approach. However, such a model is too crude to account fully for the experimental conditions; our calculations were made for an ideal molecule-cluster system. The shape of the bar-spectrum is generally very sensitive to the knowledge of the molecular motions, which themselves strongly depend on the goodness of both the potential energy model used to describe the interaction between the molecule and the cluster, and the convergence of the expansion of this potential in terms of the relevant coordinates.

Moreover, in the orientational level schemes displayed in Figure 3, additional level shifts and splittings can occur according to the v_2 vibrational state of the molecules. In effect, the potential energy surface $V_{\mathrm{M}}(\varphi, \theta, \chi)$ and the rotational constants B and C of ammonia molecules depend parametrically on the vibrational state and therefore equation (13) must be solved for both the fundamental $v_2 = 0$ and first excited $v_2 = 1$ states. As a consequence, the line frequency positions in the bar-spectrum should be slightly shifted with respect to those given in Figure 5; in particular the component lines of the pure vibration bands would not both occur at the same frequency values.

$$\mathbf{M}(\varphi,\theta,\chi)=\begin{pmatrix}\cos\varphi\cos\theta\cos\chi-\sin\varphi\sin\chi & \sin\varphi\cos\theta\cos\chi+\cos\varphi\sin\chi & -\sin\theta\cos\chi\\ -\cos\varphi\cos\theta\sin\chi-\sin\varphi\cos\chi & -\sin\varphi\cos\theta\sin\chi+\cos\varphi\cos\chi & \sin\theta\sin\chi\\ \cos\varphi\sin\theta & \sin\varphi\sin\theta & \cos\theta\end{pmatrix} \tag{A.1}$$

A last point to be commented on in this discussion concerns the relative band intensities of the spectra of Figure 5. Some bands are more intense in the calculated bar-spectrum than in the experimental one, particularly for bands at ~ 935 and ~ 960 cm^{-1}. This is due to the distribution of the optically active ammonia molecules in the so-called R and L sites (*i.e.* $\theta=\pi$ and $\theta=0$ orientation positions). Indeed, because of its lower equilibrium energy (-80 meV), the R adsorption site should be more probable than the L one. The distribution of the optically active molecules should be different for the two sites. For instance, if the distribution $\mathcal{N}^{(\mathrm{R})}=60\mathcal{N}\%$ and $\mathcal{N}^{(\mathrm{L})}=40\mathcal{N}\%$ is introduced in the calculations, instead of the $\mathcal{N}^{(\mathrm{R})}=\mathcal{N}^{(\mathrm{L})}=50\mathcal{N}\%$ one, the bands centered around 935, 960, 968, 980 and 993 cm^{-1} would decrease by about 20% of their respective intensities, whereas the bands around 971, 996, 1014 and 1023–1043 cm^{-1} would increase by 20%.

Finally, the next step that allows a rigorous interpretation of the experimental spectrum will be the calculation of the dynamical line-shifts and line-widths which are necessary to obtain the profile spectrum. This requires the determination of the dynamical coupling between the optical modes (vibration-inversion and orientation motions) and the phonon modes (vibrations of both the cluster atoms and the molecular center of mass), as well as its introduction in a more complex procedure implying phase relaxation.

Nevertheless, it would be necessary to test our model further, by determining the bar-spectra of ammonia molecules adsorbed on argon clusters in the ν_1, ν_3 and ν_4 frequency regions. More experimental investigations using high resolution infrared spectroscopy at lower temperatures are clearly needed to give finer details of the spectra.

Fruitful discussions with Profs. G. Jolicard and J. Killingbeck, Drs. M.L. Dubernet, P. Tuckey and V. Zenevich (Observatoire), and Drs. X. Bouju and J. Humbert (LPM) are gratefully acknowledged.

Appendix A: Rotational matrix transformation and molecular dipole moment

The unitary matrix $\mathbf{M}$ characterizing the transformation from the surface absolute frame ($\mathbf{X, Y, Z}$) into the molecular one ($\mathbf{x, y, z}$) through the Euler angles φ, θ and χ is given as [28]

see equation (A.1) above.

Thus the molecular dipole moment $\boldsymbol{\mu}_{\mathrm{A}}$ and its first derivative $\partial\boldsymbol{\mu}_{\mathrm{A}}/\partial Q_\lambda$, with respect to the normal coordinate Q_λ connected to the λth vibrational mode, can be written in the absolute frame as

$$\begin{aligned}\boldsymbol{\mu}_{\mathrm{A}}&=\mathbf{M}^{-1}(\varphi,\theta,\chi)\boldsymbol{\mu}_{\mathrm{M}},\\ \frac{\partial\boldsymbol{\mu}_{\mathrm{A}}}{\partial Q_\lambda}&=\mathbf{M}^{-1}(\varphi,\theta,\chi)\mathbf{b}_{\mathrm{M}}^{\lambda},\end{aligned} \tag{A.2}$$

where $\mathbf{M}^{-1}$ is the inverse matrix of $\mathbf{M}$, $\boldsymbol{\mu}_{\mathrm{M}}$ and $\mathbf{b}_{\mathrm{M}}^{\lambda}$ are the molecular dipole moment and its first derivative, with respect to the normal coordinate Q_λ, expressed in the molecular frame.

So, for the ν_2 vibrational mode, the first derivative of the molecular dipole moment with respect to the normal coordinate Q_2 is written as

$$\frac{\partial\boldsymbol{\mu}_{\mathrm{A}}}{\partial Q_2}=b_{\mathrm{M}}^{\nu_2}\left(\cos\varphi\sin\theta\ \mathbf{X}+\sin\varphi\sin\theta\ \mathbf{Y}+\cos\theta\ \mathbf{Z}\right), \tag{A.3}$$

where $b_{\mathrm{M}}^{\nu_2}=-4.405$ DÅ^{-1}. Note that only the z component of the dipole moment of the molecule (in its frame) depends on the normal coordinate Q_2. Then, in the absolute frame, the orientational squared transition elements are

$$\begin{aligned}&\left|\left\langle jmk\left|\frac{\partial\boldsymbol{\mu}_{\mathrm{A}}}{\partial Q_2}\right|j'm'k'\right\rangle\right|^2\\ &\qquad=b_{\mathrm{M}}^{\nu_2 2}\begin{Bmatrix}|\langle jmk\,|\cos\varphi\sin\theta|\,j'm'k'\rangle|^2\\ +|\langle jmk\,|\sin\varphi\sin\theta|\,j'm'k'\rangle|^2\\ +|\langle jmk\,|\cos\theta|\,j'm'k'\rangle|^2\end{Bmatrix}.\end{aligned} \tag{A.4}$$

References

1. F. Rohmund, F. Huisken, J. Chem. Phys. **107**, 1045 (1997).
2. T.E. Gough, M. Mengel, P.A. Rowntree, G. Scoles, J. Chem. Phys. **83**, 4958 (1985).
3. D.J. Levandier, M. Mengel, R. Pursel, J. McCombie, G. Scoles, Z. Phys. D **10**, 337 (1988).
4. D.J. Levandier, M. Mengel, J. McCombie, G. Scoles, in *Proceeding of the International School of Physics "Enrico Fermi"*, Course CVII, edited by G. Scoles (North-Holland, Amsterdam, 1990).
5. D.J. Levandier, S. Goyal, J. McCombie, B. Pate, G. Scoles, J. Chem. Soc. Faraday Trans. **86**, 2361 (1990).
6. X.J. Gu, D.J. Levandier, B. Zhang, G. Scoles, D. Zhuang, J. Chem. Phys. **93**, 4898 (1990).

7. S. Goyal, G.N. Robinson, D.L. Schutt, G. Scoles, J. Phys. Chem. **95**, 4186 (1991).
8. F.G. Amar, S. Goyal, D.J. Levandier, L. Perera, G. Scoles, in *Clusters of Atoms and Molecules II*, edited by Hellmut Haberland (Springer-Verlag, Paris, 1994).
9. S. Goyal, D.L. Schutt, G. Scoles, J. Chem. Phys. **102**, 2302 (1995).
10. J.P. Visticot *et al.*, Chem. Phys. Lett. **191**, 107 (1992).
11. A. Lallement *et al.*, Chem. Phys. Lett. **189**, 182 (1992).
12. D. Eichenauer, R.J. Le Roy, J. Chem. Phys. **88**, 2898 (1988).
13. L. Perera, F.G. Amar, J. Chem. Phys. **93**, 4884 (1990).
14. M.-P. Gaigeot, P. de Pujo, V. Brenner, Ph. Millie, J. Chem. Phys. **106**, 9155 (1997).
15. F. Huisken, M. Stemmler, J. Chem. Phys. **98**, 7680 (1993).
16. C. Girardet, A. Lakhlifi, J. Chem. Phys. **83**, 5506 (1985).
17. A. Lakhlifi, C. Girardet, J. Mol. Spectrosc. **116**, 33 (1986).
18. C. Girardet, A. Lakhlifi, Chem. Phys. **110**, 447 (1986).
19. A. Lakhlifi, C. Girardet, J. Chem. Phys. **87**, 4559 (1987).
20. C. Girardet, A. Lakhlifi, J. Chem. Phys. **91**, 1423 (1989).
21. C. Girardet, A. Lakhlifi, J. Chem. Phys. **91**, 2172 (1989).
22. A. Lakhlifi, S. Picaud, C. Girardet, A. Allouche, Chem. Phys. **201**, 73 (1995).
23. J.P.K. Doye, D.J. Wales, M.A. Miller, J. Chem. Phys. **109**, 8143 (1998).
24. J. Farges, M.F. de Feraudy, B. Raoult, G. Torchet, J. Chem. Phys. **84**, 3491 (1986).
25. J.A. Northby, J. Chem. Phys. **87**, 6166 (1987).
26. J.P.K. Doye, D.J. Wales, R.S. Berry, J. Chem. Phys. **103**, 4234 (1995).
27. D.J. Wales, J.P.K. Doye, J. Phys. Chem. A **101**, 5111 (1997).
28. M.E. Rose, *Elementary Theory of Angular Momentum* (Wiley, New York, 1967).
29. A. Lakhlifi, C. Girardet, J. Mol. Struct. **110**, 73 (1984).
30. A. Lakhlifi, Internal Report, 1995.
31. C.H. Townes, A.L. Schawlow, *Microwave Spectroscopy* (McGraw-Hill, London, 1955).
32. J.M.L. Martin, T.J. Lee, P.R. Taylor, J. Chem. Phys. **97**, 8361 (1992).
33. J.D. Swalen, J.A. Ibers, J. Chem. Phys. **36**, 1914 (1962).
34. J.C. Light, I.P. Hamilton, J.V. Lill, J. Chem. Phys. **82**, 1400 (1985).
35. M.L. Klein, J.A. Venables, *Rare Gas Solids* (Academic Press, London, 1976), Vol. I.